INTERNATIONAL JOURNAL OF
ENERGY AND ENVIRONMENT

Volume 8, Issue 3, 2017 pp.239-252
Journal homepage: www.IJEE.IEEFoundation.org

Experimental and numerical investigation of temperature distribution through shell and helical coil tube heat exchanger using Lab VIEW as a data acquisition program. Part I: Model validation

Vinous M. Hameed, Ahmed R. Al-Khafaji

Mechanical Engineering Department, College of Engineering, Al-Nahrain University, Baghdad, Iraq.

Received 20 Oct. 2016; Received in revised form 12 Dec. 2016; Accepted 28 Dec. 2016; Available online 1 May 2017

Abstract
Water-water shell and helical coil tube heat exchanger was used in this study. The shell was made from perplex material of length 1000mm and 150mm diameter. The coil tube was made of Cu material; it's formed in coil shape with length of 800mm and inner diameter of 90mm. The helical coil pitch is (32.7) mm. Hot and cold water tanks with heater for each side were used to reach the required water temperature for shell and helical coil tube at (35 and 65) ^{o}C respectively. Different mass flow rates had been selected in shell and tube sides (6, 8, 10, 12 L/min for each side). The data of the rig recorded by using data acquisition computer with prepared a Lab VIEW program which is built specially for this case study. A numerical analysis had done by using ANSYS-Fluent V.16 to predict the results of what had done experimentally. A very good matching of the experimental results with numerical analyses was found in this research.

Keywords: Heat exchanger; Shell and helical tube; Experimental; Numerical; CFD.

1. Introduction
A heat exchanger is a device used to transfer thermal energy efficiently between hot and a cold fluid flow in thermal contact (more than two fluid flow is also possible). In most cases the heat exchanged through intermediate metallic wall without moving part. Heat exchangers are used for the objective of (heating/ cooling) where a flowing fluid or (evaporation / condensing) of a (single / multi component) fluid stream. Other important objective of using heat exchanger is: to recover or reject heat to atmosphere. In few H.E the incoming streams (hot, cold) are exchanging temperature while directly contacted. In H.E exchanging heat happened across a separating wall (without fluids mixing). The well-known shell and tube heat exchanger are widely used in industry for its compactness [1]. Typical industrial application of heat exchanger in the following fields [2]:
-Power plant: electric power generation station use H.E for stream generation.
-Refrigeration and air conditioning: refrigerators based on evaporation- compression cycle works by the aid of two H. E. One is used for freezer cooling and the other is used to transfer heat to the surrounding air.

-Automotive: every I.C engine is equipped with a radiator to cool the engine by transferring heat to water and finally the heat is dissipated to air. Lubrication oil cooling occurs in another heat exchanger.
-Chemical processing.
-All electrical and electronic equipment supplied with a heat exchanger for their cooling.
-Oil refinery.
-Food industry: chemical processing plant and food processing plant are all involve the use of one sort or other H.E.
-Nuclear reactors (water boiling need some sort of H.E).
-Building heating and cooling require heat exchangers.
H.E compactness is so important in all application at least for economic reasons. The compaction factor is defined as the ratio of heat exchange surface area to the available volume where heat exchanges. The H.E is of compact type with low cost advantage is preferred when the installation space is a vital issue.
In order to reduce the size of a heat exchanger and improve the heat transfer efficiency, there are mainly two methods to enhance heat transfer: active and passive techniques.
*In the active heat transfer enhancement technique an external force is required to vibrate the fluid / surface or an external electric field is supplied to magnetize the fluid.
*In the passive technique heat transfer enhancement could be achieved either by fluid additives or by using a surface geometry.
Helical tube had been introduced as a H.E with advantage of high heat transfer efficient as compared with straight tube H.E. The centrifugal force generated in the helix curvature will help to produce fluid mixing by secondary flow and hence enhancement of heat transfer rate as shown in Figure 1, [3].
The secondary flow of the water inside the helical coil (due to centrifugal effect) promote the rate of heat transfer with the fluid in the shell more effectively than in straight tube and shell H.E, Figure 2 shows the schematic of helical tube and shell H.E. The secondary flow intensity is a function of coil geometry (diameters and coil pitch) [4].

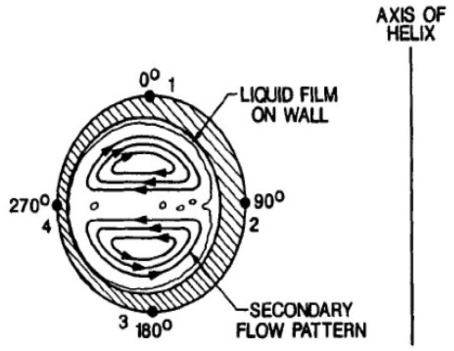

Figure 1. Secondary flow pattern in helical coils.

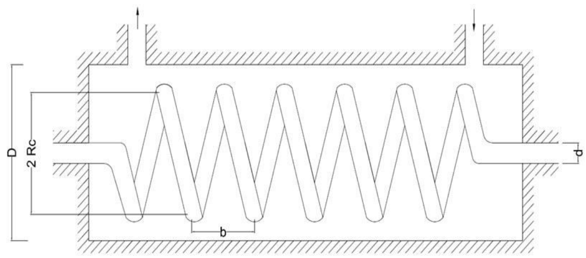

Figure 2. Shell and helical tube H.E.

Pramod S. et al. [5] performed a numerical analysis about helical tube heat exchanger by depending on tube diameter variation. Diameter of helical shape is 200mm, tube length is 2m, water is the working fluid, the average temperature was (60, 30) ^{o}C for hot and cold water respectively. The variation of internal tube diameter are (8, 10 and 12) mm respectively. The analysis depends on computing the enhanced heat transfer coefficient at each value of internal tube diameter verses some dimensionless parameters such as Reynolds number, Nusselt number, Dean Number and Helix number. This research concludes that helical coil is more efficient when Reynolds number is low. Also it is desirable to select high tube diameter and low coil diameter so this tends to increase the intensity of developed secondary flow which increases Nu. Angelo Zarrella and Michele De C. [6] had done a numerical analysis on helical coil heat exchanger that was used with ground surface heat pump. This investigation supposed a neglected effect for heat transfer in axial direction of heat exchanger and took the environment condition over surface in consideration. This study depended on performed application that was applied actually to be used in low heating and cooling capacities for homes. The results presented a good matching between numerical model and experimental work. It was found that there was no affect for the pitches of helical turns for a long time of usage. Shiva K. et al. [7] performed a numerical study about using helical coiled tubular heat exchanger and water as working fluid. Constant wall temperature was considered as boundary condition for this study. A validation has been done with other researches that presented good correlation. Also, a comparison with another simulation that used a straight tube heat exchanger has been done. The performed results showed there was an increase in heat transfer rate for 11% in the coiled tube more than that of straight tube. Also, there was an enhancement of heat transfer about 10% for coiled tube more than straight one. R. Thundil et al. [8] performed a numerical study of helical coiled heat exchanger has been performed to study its performance under certain conditions. Commercial ANSYS CFX software had selected to do this study. Two different diameters for tube were selected so they were (30 and 60) mm. water was selected as working fluid; k-є formula has been chosen to solve the turbulence in tube side. It was found that increasing in Nu number in direct proportion to pressure drop at tube side. The heat removed from tube side was the same in the two cases of diameters. Also, there was an increasing in Nusselt number for 60mm diameter more than 30mm, the ratio of Nusselt number to Dean Number was more for 60mm tube diameter than 30mm. J.S.Jayakumar et al. [9] performed an experimental and numerical investigation of helical coiled heat exchanger. Water was used as a working fluid in this investigation. Constant heat flux and constant temperature of wall were not applicable because they were not giving good satisfaction with numerical analysis. Transported media properties of heat exchanger were depended in the analysis. A numerical analysis has been done to simulate the experimental part by using FLUENT 6.2. The numerical analysis gave good predication with experimental results. Ahmed M. Elsayed [10] had done an experimental and numerical analysis investigation of studying helical coil small tube heat exchanger performance by using R-134a as working fluid so this one is used in cooling system as evaporator. Coil diameters were in the range of (30 to 60) mm while the tube diameters were in the range of (2.8 to 1.1) mm. The experimental results explained that decreasing tube diameter tends to increase boiling heat transfer coefficient up to 58% also, decreasing coil diameter increases the boiling heat transfer coefficient up to 130%. The theoretical part of this work was tended to use mathematical model that depended on the geometry of helical coil to do the optimization for them and the results showed that; for the same heat exchanger length; better performance was noticed at larger tube diameter and vice-versa so the reason was due to high pressure drop in small tube diameter. CFD process was conducted by using nano fluid for straight tube and helical tube heat exchanger so Al_2O_3 was mixed with pure water. CFD results showed an enhancement in the heat transfer coefficient up to 350% in laminar flow regime and less in turbulent flow regime as compared to pure water for same tube type. Karima E. Amori et al. [11] performed a numerical, experimental and theoretical study about some parameters in helical coil heat exchanger that was used in storage tank in solar system. The studied parameters included the water average temperature, pressure drop, friction factor, the heat rejected from coils to shell side and heat exchanger effectiveness. Many experimental and numerical results were extracted from this study that referred to a weak variation of temperature difference across the collector inlet and outlet during the test day for higher values of circulating flow rates. The circulation rate is a significant parametric affecting on the useful heat gain of the collector. The maximum heat gain was (1750W) at (12:00PM) for (9 L/min). The efficiency of the collector increases with the increase of circulation mass flow rate. High values of collector efficiency are obtained since the distribution of the triple helical coils within the shell assists to reject heat to the shell side and allows the fluid to return cooler to the collectors and increases the collector efficiency, the collector efficiency range was (48% to 78%). Effectiveness of heat exchanger is increased when circulation flow rate is decreased. The heat exchanger effectiveness follows the solar radiation, Inside Nusselt number increases with increasing Dean Number therefore increasing of tube diameter to coil diameter ratio leads to increase Nusselt number. The transition from laminar to turbulent flow is found for high circulation flow rates namely (6 and 9 L/min). For circulation flow rate of (6 L/min) the transition from laminar to turbulent flow is indicated for outer coil faster than central coil, while the flow was laminar in inner coil. For circulation flow rate of (9 L/min) the transition from laminar to turbulent is shown for all coils, but the turbulent flow starts in the outer then the central and finally in the inner. The hourly pressure drop decreases when Dean number increases for each circulation flow rate. The water density and viscosity decreases with increasing solar radiation which leads to increase the Dean number with day hours. The friction factor inside helical coiled tube increased when flow rate of circulation decreased. Vinodkumar K. et al. [12] performed an experimental and numerical investigation of using helical coil heat exchanger has been done. The objective of this study was the improvement of heat transfer coefficient in shell side and enhancement of heat transfer. Pure water and Nano-fluid (water and Al_2O_3) were the working fluids in experimental and numerical study. The analyzed and experimented study has been satisfied and they referred to increasing in net heat transfer rate by adding Nano particles i.e. (0.5 to 2) % and this tended to enhance heat transfer coefficient in shell side.

2. Experimental work

The experimental rig is constructed by assembling all the required parts as shown in the block diagram Figure 3.

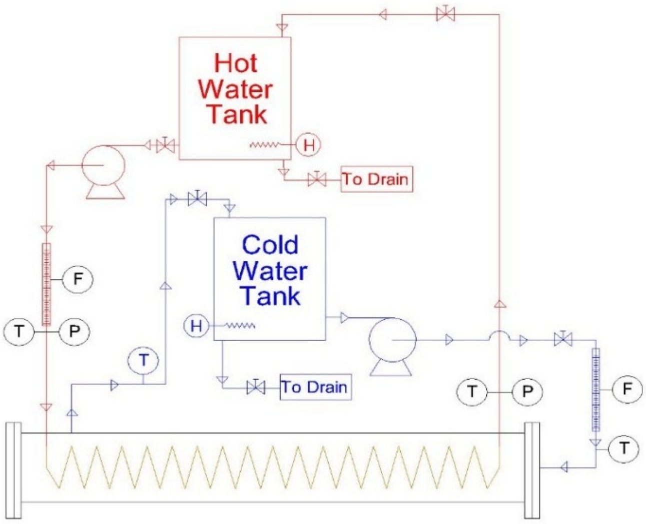

Figure 3. Schematic diagram of test rig, T: Thermocouple; P: Pressure gage; F: Routameter; H: Heater.

2.1 Insulated shell and helical coil heat exchanger

The test section consists of two parts. The first part is an insulated tube which has been manufactured from Perspex material of (150mm) inner diameter, (1000mm) length and (1mm) thickness. The second part is copper tube. The smooth copper tube is (12.7mm) as outer diameter. So this tube is coiled to form a coil diameter as (90mm) while its length is (800mm). The first time straight tube was installed. Then the coil tube was installed. Pitch distance is set at 32.7mm as shown in Figure 4.

The Perspex shell was closed from both ends by special machine flanges. All the flanges contain eight holes which connect the flanges together which fitted the end side of the shell. Circle channel for a rubber O-ring with thickness (6mm), diameter (175mm). Each O-ring is adopted in a circular groove with depth (2mm) inside each flange was designed to prevent flange water leakage, as shown in Figure 5.

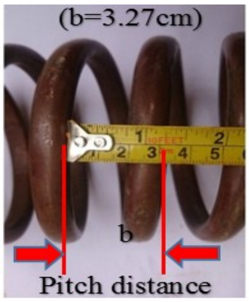

Figure 4. Helical coil pitch.

Figure 5. Flangs of heat exchanger.

Thermocouples are distributed by equal distance over the length of shell to measure water temperature. The other thermocouples were fixed on the inlet and outlet of shell and tube side to measure the entered and exit temperature of hot and cold water. Bourdon gages are fixed on inlet and outlet of tube side to measure the pressure difference between inlet and outlet water from tube as shown in Figure 6.

The shell and tube heat exchanger is designed for counter flow configuration, in which the hot water flows in the tube in opposite direction to the cold water which flows in shell side.

2.2 Water tanks

Two water tanks are adopted to join with tube and shell side respectively to provide hot and cold water for heat exchanger. Each water tank fitted with an electrical heater (3000W) to raise the water temperature. The required set point temperature of cold water tank at 35°C and for the hot source is 65°C.

Figure 6. Bourdon gages position.

2.3 Pipe connection and valves

CPVC pipes are used to connect the heat exchanger with water tanks to complete the water cycle in shell and tube side. These pipes have the ability to resist 10000 kPa pressure and up to 80 ^{o}C temperature. The used CPVC pipe diameter in rig is 6.25mm. With suitable valves to control the flow.

2.4 Centrifugal pump

Pumping cold or hot water to heat exchanger is done by means of two centrifugal pumps. The used pumps are characterized with the following specifications Table 1.

Table 1. Pumps specification.

Head (m)	35
Discharge (L/min)	33
Power (hp)	0.75

2.5 Flow meter

The used flow meter shown in Figure 7 has an operation range 1.8-18 L/min for tube side while 4-36 L/min for shell side. Calibrations for these flow meters were done to ensure their measurements volumetric flow rate according to the experiment operation conditions.

Figure 7. Flow meters.

2.6 Thermocouples

Eight K-type thermocouples are used in the experiment arranged along the rig to measure the temperature. These thermocouples connected to computer through an arduino card along the rig. All thermocouples used in the rig are calibrated to ensure their measurements.

2.7 Arduino card

It is a programmer electronic card that is used to record and collect the selected data. This card is used as a data acquisition in order to send and receive the data to the computer. Lab-VIEW is used with the arduino. The Arduino complete circuit consists of the components:

1. Arduino card (MEGA type). Shown in Figure 8.
2. DC source (supplied from small battery 12V, 9mA).
3. Printed electronic circuit, see Table 2.
4. Laptop with Lab-VIEW program.
5. Connection wires.
6. Support container.

The data acquisition is designed by connecting all the above components as shown in Figure 8. Figure 9 show the Lab-VIEW program display. This circuit have the ability to read the temperature distribution along the heat exchanger and send it as a signal to the computer which collect and tabulate these data and also have the ability to draw these data as a function of time. The block diagram was plotted by Lab-VIEW software, as shown in Figure 10.

Table 2. Printed electronic circuit.

NO.	Part name	Quantity
1	Electronic circuit	1
2	IC (AD595AQ) With its base	4
3	Capacitor 220 microfarad	1
4	Led light	1
5	connection	7
6	Protection IC	2

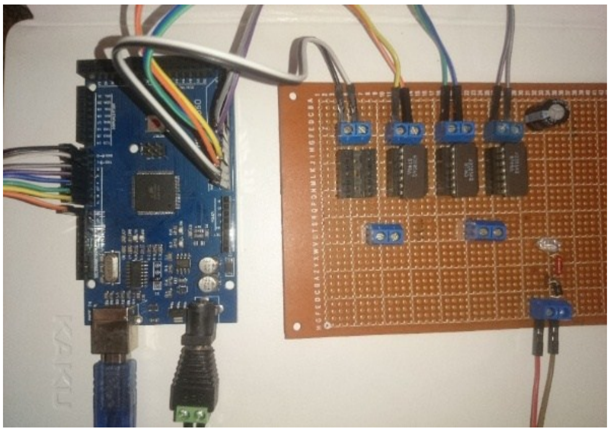

Figure 8. Data accusation circuit.

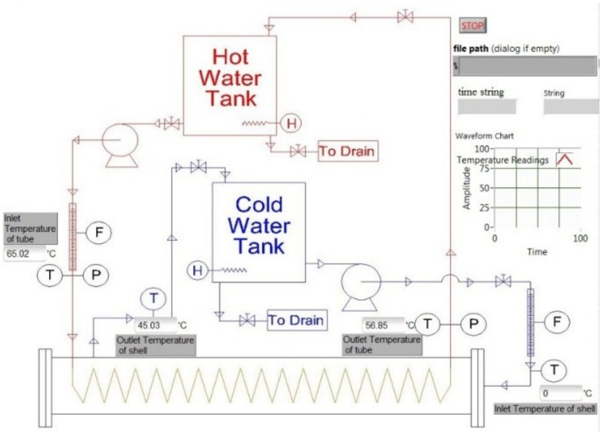

Figure 9. Lab-VIEW program.

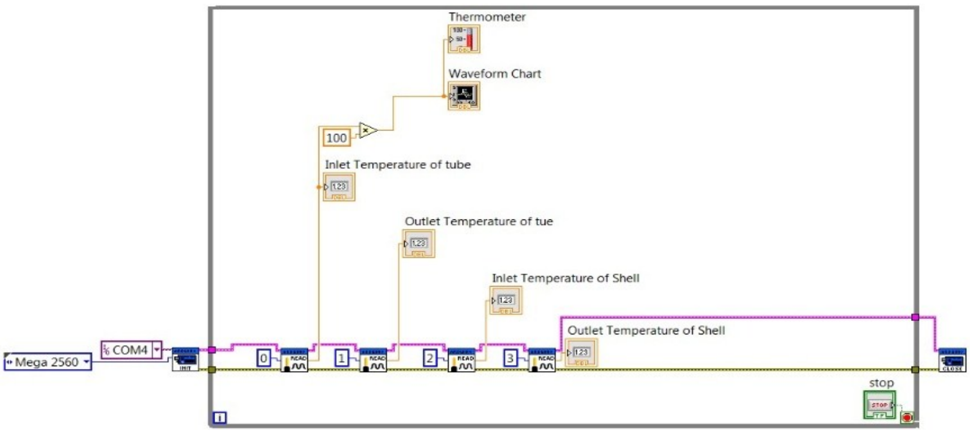

Figure 10. Block diagrame of Lab-VIEW.

3. Numerical part

The invention of high speed computers, combined with the accurate numerical methods for solving physical problems, has revolutionized the way we study and practice fluid dynamics and heat transfer problems. This is called Computational Fluid Dynamics (CFD), and it has made it possible to analyze complex flow geometries with the same ease as that faced while solving idealized problems using conventional methods. CFD may thus be regarded as a zone of study combining fluid dynamics and numerical analysis. Historically, the earlier development of CFD in the 1960s and 1970s was driven by the need of the aerospace industries. Modern CFD, however, has applications across all disciplines-civil, mechanical, electrical, electronics, chemical, aerospace technology, ocean science, and biomedical engineering being a few of them. CFD substitutes analytical studies and experimental testing, and reduces the total time of testing and designing [13].

3.1 Geometry creation

ANSYS designing modeler used to draw the geometries of this work which consist helical coil tube heat exchanger with inlet and outlet portions. The outside flow is confined by insulating tube having inlet and outlet portions as shown in Figure 11.

3.2 Mesh generation

Unstructured mesh is used in the present study to discretize the computational domain into a finite number of control volumes by using the finite–volume scheme. Structured mesh is ruled out because it is favorable for easy cases and it becomes insufficient and time consumed for complicated geometries. The model was meshed by using ANSYS-fluent computational fluid dynamic (CFD) package as shown in Figures 12-14 which are a representative of all cases because of similarity. The refinement and generation of mesh system are very crucial to predict the heat transfer in sophisticated geometries. Thus both the density and distribution of the mesh lines play distinct roles for accuracy. It's made 988,588 elements for this case (3.27cm pitch).

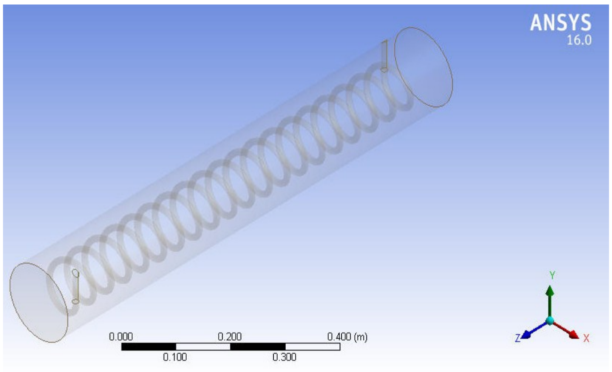

Figure 11. CFD domain of heat exchanger.

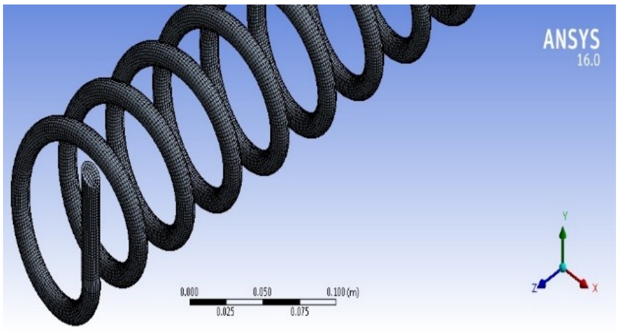

Figure 12. CFD meshing of heat exchanger.

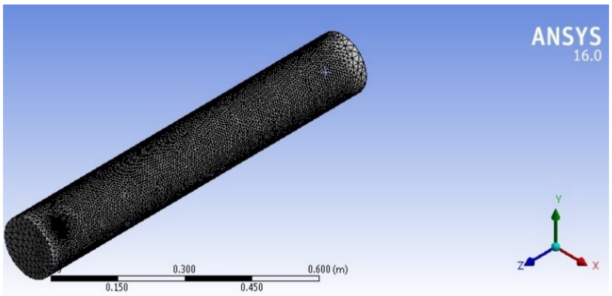

Figure 13. CFD meshing for shell.

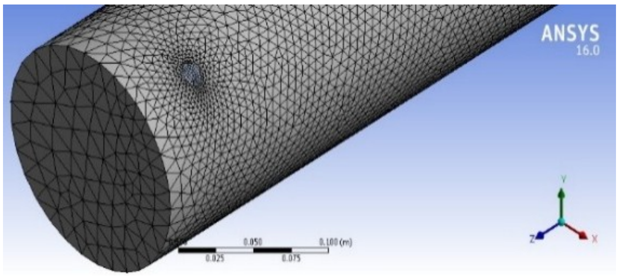

Figure 14. CFD meshing for part of shell.

3.3 Assumptions

The following assumptions are used for water during the present study:

1. Steady state. 2. Newtonian fluid. 3. Incompressible. 4. Three dimensional.
5. Turbulent flow in the coil side (tube) and Laminar flow in the Shell side.
6. Buoyancy effect is assumed to be negligible.
7. Radiation heat transfer is not considered.

3.4 Governing equations

The governing differential equation for the fluid flow is given by Continuity equation or mass conservation equation, Navier Stokes equation or momentum conservation equation and energy conservation equation [14].

1- Continuity equation:

$$\frac{\partial(\rho u)}{\partial x}+\frac{\partial(\rho V)}{\partial y}+\frac{\partial(\rho W)}{\partial z}=0 \tag{1}$$

2- Navier Stokes equation:

$$\rho\left(u\frac{\partial u}{\partial x}+V\frac{\partial u}{\partial y}+W\frac{\partial u}{\partial z}\right)=\rho X-\frac{\partial p}{\partial x}+\frac{1}{3}\mu\frac{\partial}{\partial x}\left(\frac{\partial u}{\partial x}+\frac{\partial V}{\partial y}+\frac{\partial W}{\partial z}\right)+\mu\nabla^2 u \tag{2}$$

$$\rho\left(u\frac{\partial V}{\partial x}+V\frac{\partial V}{\partial y}+W\frac{\partial V}{\partial z}\right)=\rho Y-\frac{\partial p}{\partial y}+\frac{1}{3}\mu\frac{\partial}{\partial y}\left(\frac{\partial u}{\partial x}+\frac{\partial V}{\partial y}+\frac{\partial W}{\partial z}\right)+\mu\nabla^2 V \tag{3}$$

$$\rho\left(u\frac{\partial w}{\partial x}+V\frac{\partial w}{\partial y}+W\frac{\partial w}{\partial z}\right)=\rho Z-\frac{\partial p}{\partial z}+\frac{1}{3}\mu\frac{\partial}{\partial z}\left(\frac{\partial u}{\partial x}+\frac{\partial V}{\partial y}+\frac{\partial W}{\partial z}\right)+\mu\nabla^2 W \tag{4}$$

3- Energy equation:

$$\rho c_p\left(u\frac{\partial T}{\partial x}+V\frac{\partial T}{\partial y}+W\frac{\partial T}{\partial z}\right)=\left(u\frac{\partial P}{\partial x}+V\frac{\partial P}{\partial y}+W\frac{\partial P}{\partial z}\right)+K\nabla^2 T+\mu\emptyset \tag{5}$$

Where:

$$\emptyset=2\left[\left(\frac{\partial u}{\partial X}\right)^2+\left(\frac{\partial V}{\partial y}\right)^2+\left(\frac{\partial w}{\partial z}\right)^2\right]+\left[\left(\frac{\partial u}{\partial y}+\frac{\partial V}{\partial X}\right)^2+\left(\frac{\partial V}{\partial z}+\frac{\partial W}{\partial y}\right)^2+\left(\frac{\partial W}{\partial X}+\frac{\partial u}{\partial z}\right)^2\right]-\frac{2}{3}\left[\frac{\partial u}{\partial x}+\frac{\partial V}{\partial y}+\frac{\partial W}{\partial z}\right] \tag{6}$$

$$Re=\frac{\rho_c u_c D_h}{\mu_c} \qquad [15] \tag{7}$$

$$Dh=\frac{D_o^2-\pi D_c d_o^2\gamma^{-1}}{D_c+\pi D_c d_o\gamma^{-1}} \qquad [16] \tag{8}$$

$$\gamma=\frac{b}{2\pi R_c} \qquad [16] \tag{9}$$

$$q_c=m_c cp_c(T_{co}-T_{ci}) \qquad [15] \tag{10}$$

$$q_h=m_h cp_h(T_{ho}-T_{hi}) \qquad [15] \tag{11}$$

$$h_i=\frac{q_h}{A_i(T_m-T_s)} \qquad [15] \tag{12}$$

$$T_s=\frac{T_{s1}+\cdots+T_{s8}}{8} \qquad [15] \tag{13}$$

$$T_m=\frac{T_{hi}+T_{ho}}{2} \qquad [15] \tag{14}$$

$$Nu=\frac{h_i d_i}{k_h} \qquad [15] \tag{15}$$

$$h_o=\frac{q}{A_o LMTD} \qquad [15] \tag{16}$$

$$LMTD=\frac{\Delta T_2-\Delta T_1}{ln\left(\frac{\Delta T_2}{\Delta T_1}\right)}=\frac{\Delta T_1-T_2}{ln\left(\frac{\Delta T_1}{\Delta T_2}\right)} \qquad [15] \tag{17}$$

$$\Delta T_1 = T_{hi} - T_{co} \quad [15] \tag{18}$$

$$\Delta T_2 = T_{ho} - T_{ci} \quad [15] \tag{19}$$

$$\varepsilon = \frac{q_{act}}{q_{max}} \quad [15] \tag{20}$$

$$q_{max} = m^{\cdot}_{min} cp(T_{hi} - T_{ci}) \quad [15] \tag{21}$$

$$q_{act} = m^{\cdot} cp\,(T_o - T_i) \quad [15] \tag{22}$$

3.5 Boundary conditions

Velocity inlet was specified for shell and tube sides during this study. On the other hand the temperature inlet of the tube side is (65°C) while in shell side is (35°C), and the outer shell wall is supposed perfectly insulated.

3.6 Working fluid and material properties

It was tended to use software package EES Engineering Equation Solver to get any required data for water and cupper. This package is considered by most of thermodynamics reference book such as Younos to get the required properties. The properties of cold and hot water at (35 and 65) °C respectively The tube of the heat exchanger was made up of copper alloy for maximizing the heat transfer, because copper alloy has good thermal conductivity. Also the properties of the copper alloy were also remains constant throughout the analysis.

4. Results and discussion

The results are obtained three parts as show below:

4.1 Experimental data descriptions

Optimization of heat exchanger design requires intensive studies of the process variables especially those enhancing heat transfer, which is the major objective of this valuable piece of equipment. In this study the main key variable in the process was mass flow rate (for the helical coil tube and shell tube counter flow). The flow rates that selected in this study are (6, 8, 10 and 12) L/min for each side, that's mean there are 16 run in this case. In each run the data taken by using the Lab VIEW program. The following figures are obtained which represented the temperature difference or amount of heat lose by the helical coil tube of the heat exchanger which vary according to hot water mass flow rates for each cold water mass flow rate. The same procedure are applied for different Re numbers in the shell side to show their effect on the amount of heat or temperature gain by the cold fluid (water) as shown in the following figures.

Figure 15 shows the relation between Re_h and ΔT_h (T_{ho}- T_{hi}) for certain water flow rate in the shell side which is represented as a cold fluid. The increase of hot water flow rate in the helical coil tube will decrease the amount of heat gain by it which is function of temperature difference in tube side for certain water flow rate in the shell side. Also, for certain water flow rate in the tube side while the water flow rate in the shell side will change the increase of cold water (shell side) flow rate will increase the amount of heat gain by the cold fluid.

Figure 16 shows the amount of heat gain by the cold water for increasing the flow rate of shell side water flow rate where the curve shows an inverse relation between them for a certain flow rate in the hot helical coil water. The amount of exit temperature increase is largely affected by the contact time between the two fluids and this fact is clearly appearing by the behavior of the curve. Increasing the hot water (in the helical coil) flow rate for certain cold water (shell side) flow rate will increase the outlet temperature of the cold fluid and as a result the amount of heat gain by the cold fluid.

4.2 Numerical validation

Figures 17, 18 shows the experimental and numerical validation in the temperature difference through the helical coil tube for mass flow rate (6 and 12) L/min in the shell side and (6, 8, 10, and 12) L/min for the helical coil tube side.

The Numerical analysis gives a very well matching with the experimental results (approach to 2.87 % error) as explained in Figure 17 and 18. It's clear that the error is highest in the low mass flow rate and its decrease gradually with the mass flow rate increase. This behavior due to the error of experimental measurement devices.

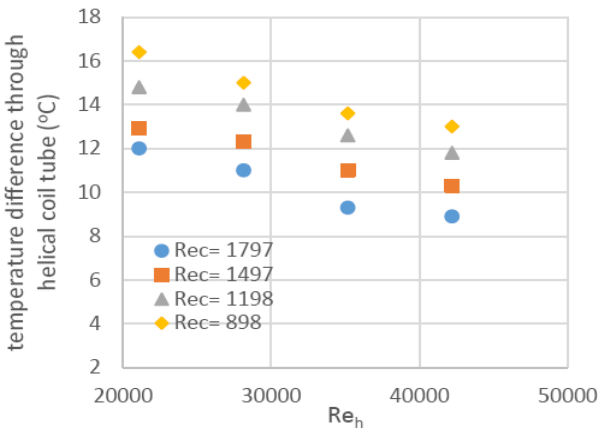

Figure 15. The relation between hot water temperature difference and Re_h for different Re_c.

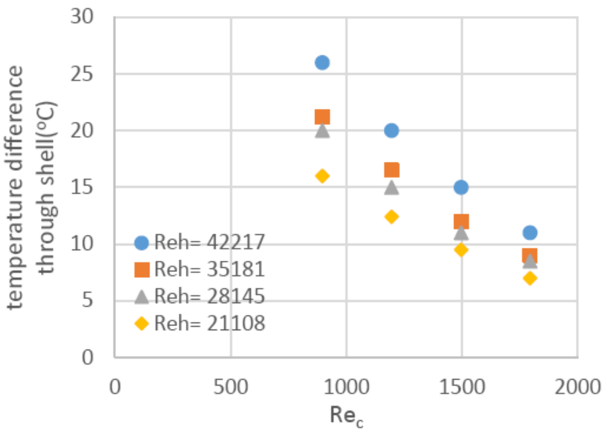

Figure 16. The relation between cold water temperature difference and Re_c for different Re_h.

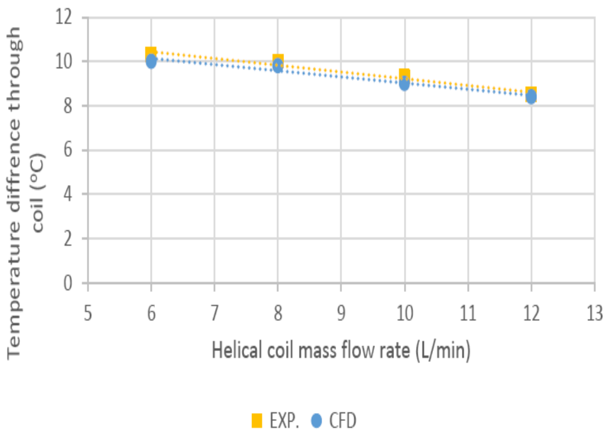

Figure 17. Validation of numerical and experimental results for shell flow rate 6 L/min and helical coil flow rate (6, 8, 10, 12) L/min.

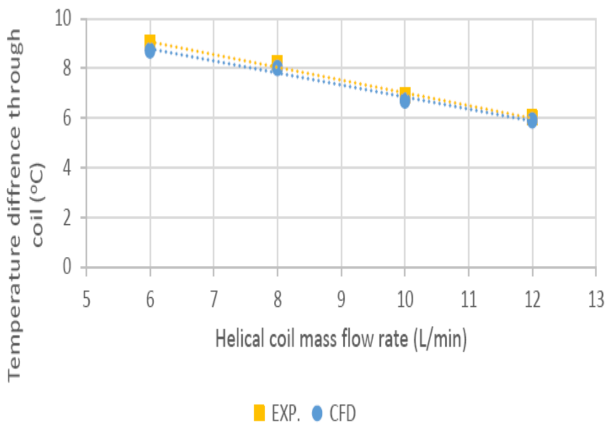

Figure 18. Validation of numerical and experimental results for shell flow rate 12 L/min and helical coil flow rate (6, 8, 10 and 12) L/min.

4.3 Numerical analysis

The results of numerical simulation by using ANSYS-Fluent computational fluid dynamic (CFD) package model are presented to show both the flow field and heat transfer distribution along a helical coil heat exchanger of the present models. Two flow rates value are selected, there are (6 and 12) L/min for the hot and cold water sides (4 runs will show in this study).

The following contours are obtained showing the temperature distribution profiles in the following figures. Figures 19 and 20 clearly show the amount of heat supplied and the temperature profile for the case of cold water flow rate 6 L/min and hot water flow rate of 6 and 12 L/min respectively.

Figures 21 and 22 show the amount of heat supplied and the temperature profile for the case of cold water flow rate 12 L/min and hot water flow rate of 6 and 12 L/min respectively:

ANSYS shows clearly the temperature distribution through the helical coil heat exchanger and the most effecting flow rate on increase its effectiveness. Its clearly shown that the heat exchange decrease with the increase of hot and cold water flow rate

A radial temperature distribution is also investigated for the same four cases the same distance from the cold water entrance =0.3 and 0.7m respectively and the following figures are obtained as shown in Figures 23 to 30.

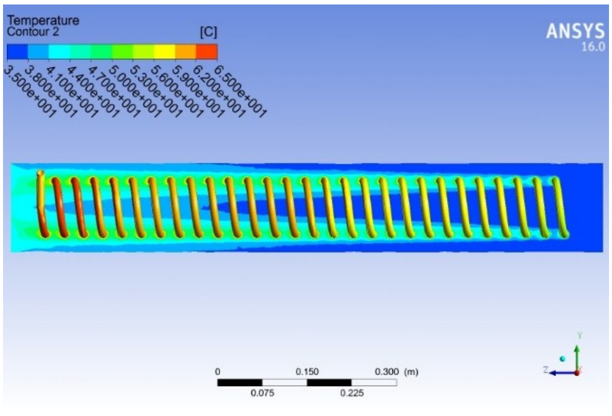

Figure 19. Temperature contours (distribution) at Re_c=898.404, Re_h=21108.98.

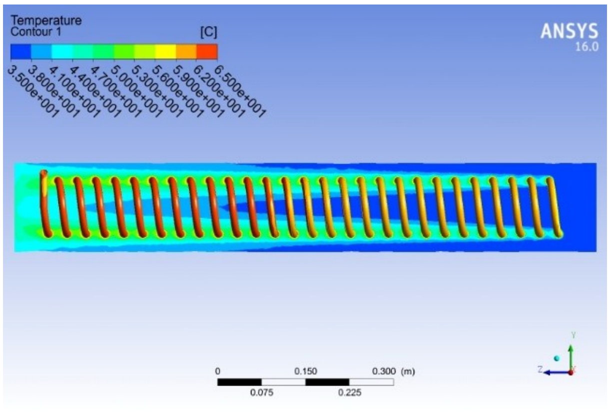

Figure 20. Temperature contours (distribution) at Re_c=898, Re_h=42218.

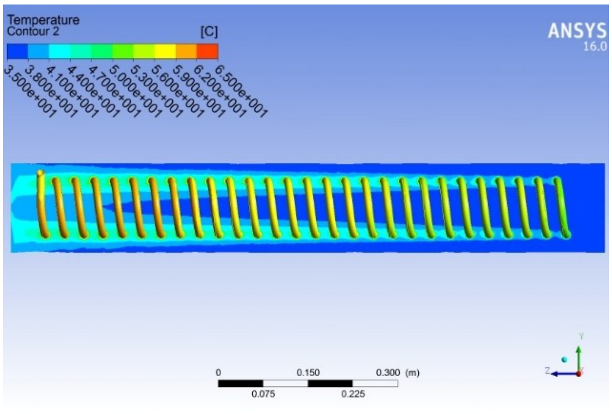

Figure 21. Temperature contours (distribution) at Re_c=1796, Re_h=21108.

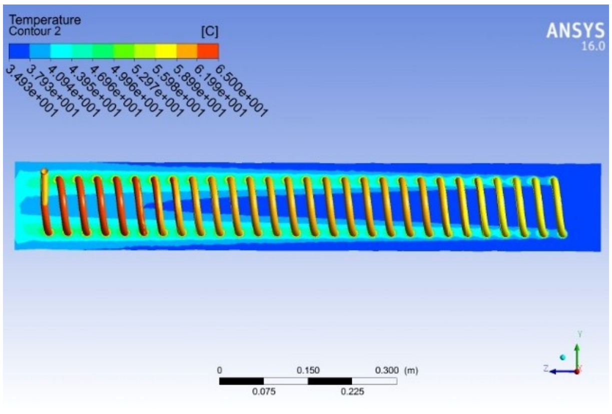

Figure 22. Temperature contours (distribution) at Re_c=1796 Re_h=42218.

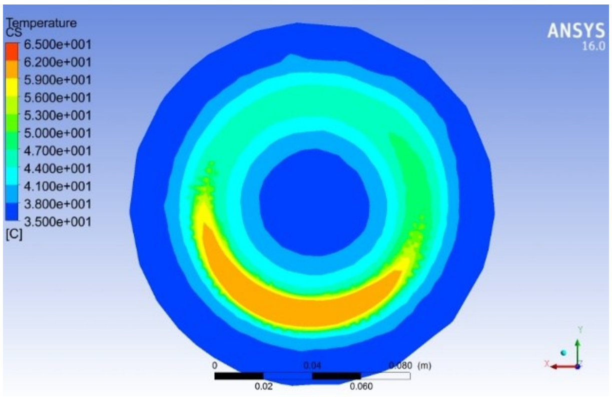

Figure 23. Temperature contours (Cross section at 0.3m from the inlet) at Re_c=898.404, Re_h=21108.98.

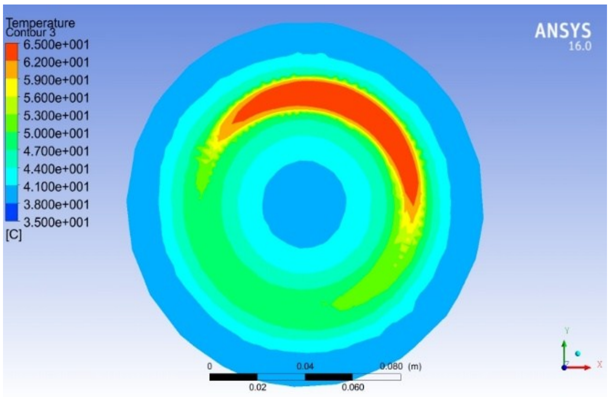

Figure 24. Temperature contours (Cross section at 0.7m from the inlet) at Re_c=898.404, Re_h=21108.98.

In comparing Figures 23 and 24; it's clear that the amount of heat gain by the cold water and the temperature distribution of the hot cold water near the helical coil and far from it.
By comparing Figures 23 and 25 the effect of increasing Reynold number is appeared clearly from the contours of heat distributed radially through the shell. Same thing is for Figure 25 compared with Figure 27.

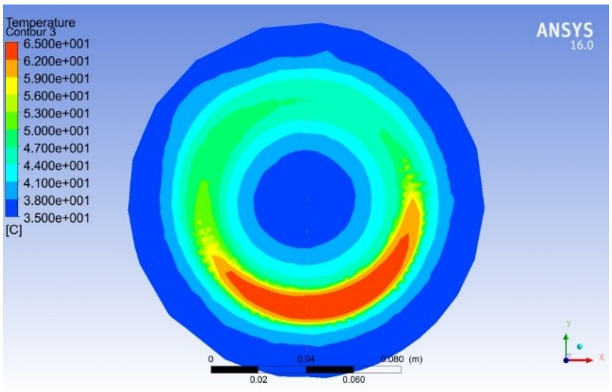

Figure 25. Temperature contours (Cross section at 0.3m from the inlet) at Re_c=898.404, Re_h =42218.

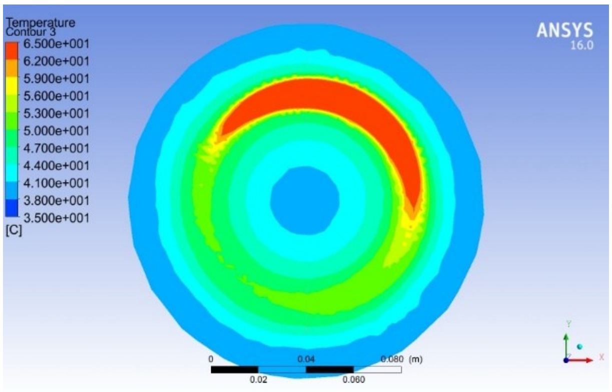

Figure 26. Temperature contours (Cross section at 0.7m from the inlet) at Re_c=898.404, Re_h =42218.

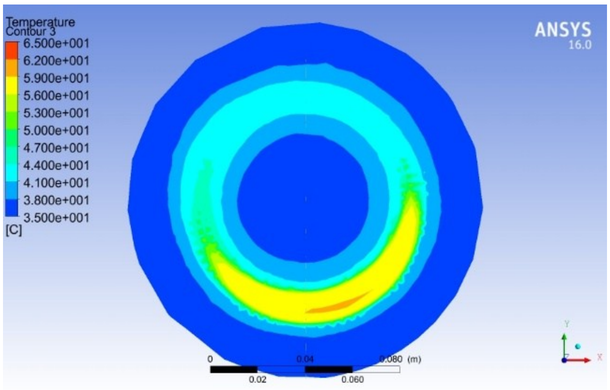

Figure 27. Temperature contours (Cross section at 0.3m from the inlet) at Re_c=1796, Re_h =21108.98.

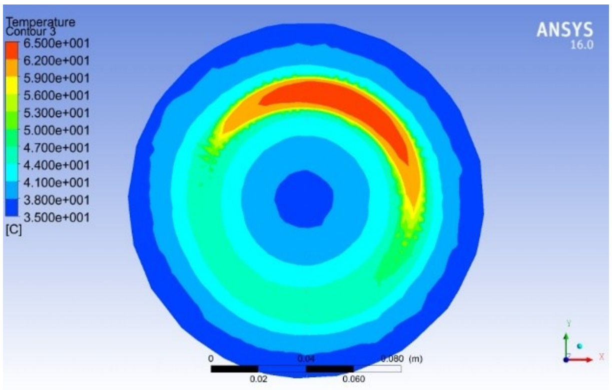

Figure 28. Temperature contours (Cross section at 0.7m from the inlet) at Re_c=1796, Re_h =21108.98.

The effect of increasing the flow rate of cold fluid can be seen by comparing Figures 23 with 27 and Figures 26 with 28 respectively for the same hot water flow rate (tube side).

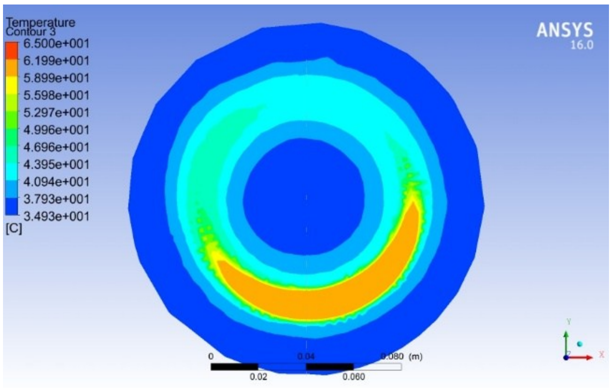

Figure 29. Temperature contours (Cross section at 0.3m from the inlet) at Re_c=1796, Re_h =42218.

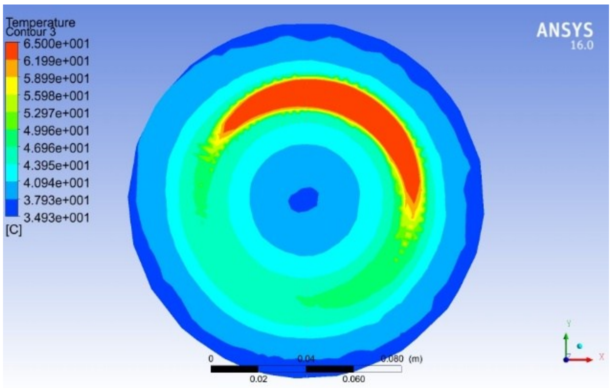

Figure 30. Temperature contours (Cross section at 0.7m from the inlet) at Re_c=1796, Re_h =42218.

The same comparison between Figures 25 with 29 and 26 with 30 can be done to discover the effect of increasing the cold fluid (shell side) flow rate.
Also, a maximum heat contours can be specified at the low hot water flow rate (in the helical coil tube) and maximum flow rate of the cold water (at the shell side) in the region far from the entrance of cold water as shown in Figure 30.

5. Conclusion

- It's clear that there are well matching results between the experimental and numerical results (approach to 2.87% error) as approved in the Figures 17 and 18.

These results of temperatures distribution are recorded by the Lab VIEW software which provides an accurate complete control helical coil heat exchanger supported by a numerical investigation of the temperature profile of that type of heat exchanger by using CFD.

- For certain tube water flow rate the increase of cold water (shell side) flow rate will increase the amount of heat gain by the cold fluid.
- Increasing the mass flow rate in the tube side for the same shell flow rate will increase the exit water temperature.

Nomenclature

H.E	Heat Exchanger	***b***	Pitch length
D_c	Inner coil diameter	*Q*	Mass flow rate
R_c	radius	*q*	Amount of heat transfer
D_i	Inner diameter of inner tube area	*T*	Temperature
D_o	Outer diameter of inner tube area	T_{ci}	inlet temperature of cold fluid
D_h	Hydraulic diameter	T_{co}	Outlet temperature of cold fluid
d_i	Inner coil diameter	T_{hi}	Inlet temperature of hot fluid
d_o	Outer coil diameter	T_{ho}	Outlet temperature of hot fluid
F	friction factor	T_s	Temperature of tube surface
Nu	Nusselt number (h d / k)	$\mathcal{E}$	Effectiveness
Re	Reynolds number	*CFD*	Computational fluids dynamics
P	Pressure	*LMTD*	Long mean temperature difference

References

[1] Arthur E. Bergles, "The Imperative to Enhance Heat Transfer", Department of Mechanical Engineering, Aeronautical Engineering and Mechanics Rensselaer Polytechnic Institute pp.13-29, 1999.

[2] Madhuri Tayde, Jeevan Wankhade and Shylesha Channapattana "Heat Transfer Analysis of a Helically Coiled Heat Exchanger", ijird, ISSN 2278 – 0211, 3 (13), pp. 265-268, December 2014.

[3] Ralph L. Webb and Nae Hyun Kim, "principles of enhanced heat transfer", Tylor and francis group, 2005.

[4] Soumya Ranjan Mohanty and A. K. Satapathy, "CFD Analysis of Heat Transfer in A Helical Coil Heat Exchanger Using FLUENT", B.Sc Thesis, National Institute of Technology.

[5] Pramod S. Purandarea, Mandar M. Leleb, Rajkumar Guptac, "Parametric Analysis of Helical Coil Heat Exchanger", IJERT, 1 (8), pp. 01-05, October 2012.

[6] Angelo Z. and Mechili D., "Heat transfer analysis of short helical borehole heat exchangers", Applied Energy journal, Elsevier, Vol. 102, pp. 1477-1491, 2013.

[7] Shiva Kumara, K.Vasudev Karantha, "Numerical Analysis of a Helical Coiled Heat Exchanger using CFD", IJTT, 3 (4), pp. 126-130, December 2013.

[8] R. Thundil Karuppa Raj, Manoj Kumar S., Aby Mathew C. and T. Elango, "Numerical Analysis of Helically Coiled Heat Exchanger Using CFD Technique", ARPNJEAS, 9 (3), pp. 300-307, March 2014.

[9] J.S. Jayakumar, S.M. Mahajani, J.C. Mandal,P.K. Vijayan, Rohidas Bhoi, "Experimental and CFD estimation of heat transfer in helically coiled heat exchangers", chemical engineering research and design, Elsevier 86, pp. 221-232, 2008.

[10] Ahmed Mohamed Elsayed, "Heat Transfer in Helically Coiled Small Diameter Tubes for Miniature Cooling Systems", Ph.D. Thesis, University of Birmingham, 2011.

[11] Karima E. Amori Jinan Shaker Sherza, "An investigation of shell-helical coiled tube heat exchanger used for solar water heating system", ISDE, 4 (15), pp. 78-90, 2013.

[12] Vinodkumar, Kiran Voonna, T.K. Tharakeshwar, "Improvement of Heat Transfer Coefficients in a Shell and Helical Tube Heat Exchanger Using Water/Al2O3 Nanofluid", IRJET, 2 (3), pp. 853-856, 2015.

[13] Satyabrata Kanungo, “Numerical Analysis to Optimize The Heat Transfer Rate of Tube-in-Tube Helical Coil Heat Exchanger”, Department of Mechanical Engineering, National Institute of Technology Rourkela, Odisha 2014.
[14] Lars Davidson, “An Introduction to Turbulence Models”, Department of Thermo and Fluid Dynamics, Chalmers University of Technology, Sweden, 2009.
[15] Vinous M. Hameed and Bashar Muslem Essa, “Experimental and numerical investigation to evaluate the performance of triangular finned tube heat exchanger” International journal of energy and environment, 6 (6), pp.553-566, 2015.
[16] Vinous M. Hameed and Bashar Muslem Essa, “Turbulent flow heat transfer and pressure loss in a double pipe heat exchanger with triangular fins” International journal of energy and environment, 7 (2), pp. 149-158, 2016.

Vinous Majeed Hameed Al-Temimi, Asst. Proff. at Mechanical Engineering Department, College of Engineering, Al-Nahrain University, Ph.D. in Chemical Engineering College of Engineering, Al-Nahrain University, Iraq. (2004). M.Sc. in Chemical Engineering College of Engineering, Al-Nahrain University, Iraq. (1999). B.Sc. in Chemical Engineering College of Engineering, Al-Nahrain University, Iraq. (1996). Academic experience: Three chemical engineering M.Sc. students and two mechanical engineering M.Sc. students Specialization: Thermodynamics, heat transfer, solar energy, refrigeration and power cycles, enhanced heat exchangers. Seven published papers and a Fulbright scholar which is a grant from the US embassy to Delaware University at 2014. Rewards: Certificate of appreciation from the prime minister for the project of the graduation student which entitled "Solar parabola mirror for power generation 2013". Certificate of appreciation from the president of Al-Nahrain university for the final year project at Rabee Al-Nahrain Festival which entitled "Solar parabola mirror for power generation" 2013. Certificate of appreciation from the president of Al-Nahrain University for getting the second position on the graduation students at 1996; and state award for competition between the graduation chemical engineering students at 1995/1996.
E-mail address: venus.m.hameed@gmail.com

Ahmed Raad Bahlool Researcher in Thermal Engineering, Department of Mechanical Engineering, Al-Nahrain University, Iraq. B.Sc. In Mechanical Engineering, College of Engineering, University of Kufa, Iraq. Specialization: General Mechanics, Graduation Date: 2013.
E-mail address: ahmedrbm91@gmail.com

